Hemp, an mbt domain-containing protein, plays essential roles in hematopoietic stem cell function and skeletal formation

Hiroaki Honda[a,1,2], Keiyo Takubo[b,1], Hideaki Oda[c], Kenjiro Kosaki[d], Tatsuya Tazaki[a], Norimasa Yamasaki[a], Kazuko Miyazaki[a], Kateri A. Moore[e], Zen-ichiro Honda[f], Toshio Suda[b], and Ihor R. Lemischka[e]

[a]Department of Disease Model, Research Institute of Radiation Biology and Medicine, Hiroshima University, Minami-ku, Hiroshima 734-8553, Japan; [b]Department of Cell Differentiation, The Sakaguchi Laboratory of Developmental Biology, [d]Department of Pediatrics, Keio University School of Medicine, Shinjuku-ku, Tokyo 160-8582, Japan; [c]Department of Pathology, Tokyo Women's Medical University, Shinjuku-ku, Tokyo 162-8666, Japan; [e]Department of Gene and Cell Medicine, Black Family Stem Cell Institute, Mount Sinai School of Medicine, New York, NY 10029; and [f]Department of Allergy and Rheumatology, Faculty of Medicine, Graduate School of Medicine, University of Tokyo, Bunkyo-ku, Tokyo 113-8655, Japan

Edited by Owen N. Witte, The Howard Hughes Medical Institute, University of California, Los Angeles, CA, and approved December 14, 2010 (received for review March 31, 2010)

To clarify the molecular pathways governing hematopoietic stem cell (HSC) development, we screened a fetal liver (FL) HSC cDNA library and identified a unique gene, *hematopoietic expressed mammalian polycomb* (*hemp*), encoding a protein with a zinc-finger domain and four malignant brain tumor (mbt) repeats. To investigate its biological role, we generated mice lacking Hemp (*hemp*$^{-/-}$). *Hemp*$^{-/-}$ mice exhibited a variety of skeletal malformations and died soon after birth. In the FL, *hemp* was preferentially expressed in the HSC and early progenitor cell fractions, and analyses of fetal hematopoiesis revealed that the number of FL mononuclear cells, including HSCs, was reduced markedly in *hemp*$^{-/-}$ embryos, especially during early development. In addition, colony-forming and competitive repopulation assays demonstrated that the proliferative and reconstitution abilities of *hemp*$^{-/-}$ FL HSCs were significantly impaired. Microarray analysis revealed alterations in the expression levels of several genes implicated in hematopoietic development and differentiation in *hemp*$^{-/-}$ FL HSCs. These results demonstrate that Hemp, an mbt-containing protein, plays essential roles in HSC function and skeletal formation. It is also hypothesized that Hemp might be involved in certain congenital diseases, such as Klippel-Feil anomaly.

fetal liver hematopoiesis | skeletal abnormality

Stem cells are characterized by their ability to balance self-renewal activity with differentiation into mature cell lineages. Among tissue-specific stem cells, hematopoietic stem cells (HSCs) are most intensively studied and well characterized (1, 2). Functional and physiological studies have identified a number of genes that regulate and maintain HSC activity (3–5); however, the overall molecular mechanisms governing HSC function are not fully understood.

To provide insights into these mechanisms, we generated and sequenced a subtracted cDNA library from mouse fetal liver (FL), in which hematopoietic cells are produced and expanded (6). Enrichment of HSC-specific gene products after subtraction was verified by the presence of *Runx1*, *CD34*, and *flk2/flt3*, and the absence of *β-actin* and other housekeeping genes (6). The experimental procedures, primary datasets, and the results of the computational analyses are contained in the Stem Cell Database (http://stemcell.mssm.edu/v2/).

Among the genes presented in the Stem Cell Database, we identified one that encodes a protein containing a C2C2 zinc finger domain and four tandem malignant brain tumor (mbt) repeats. Mbt is a protein domain originally identified in the protein product of a *Drosophila polycomb group* (*PcG*) gene and *lethal(3)malignant brain tumor* [*D-l(3)mbt*], whose recessive mutations cause the malignant transformation of larval and adult brain tissues (7). Because the mbt repeats are also found in another *Drosophila PcG* gene, *Scm* (*sex comb on midleg*), and are highly conserved in their human counterparts, *H-l(3)mbt* (8, 9), *SCMH1* (*sex comb on midleg homolog 1*) (10), and *SCML2* (11), we named the this gene *hemp* [*hematopoietic expressed mammalian polycomb*, also deposited in the database as *mbtd1* (*mbt domain containing 1*)].

To investigate the biological roles of Hemp, we generated mice deficient in *hemp* and analyzed their general embryonic development and HSC functions.

Results

Structure and Characterization of Hemp, a Unique mbt-Containing Protein. The comparison of amino acid sequences of mouse and human Hemp proteins is shown in Fig. 1*A*. In both mouse and human, Hemp is composed of a C2C2 zinc-finger domain at the N terminus (circled), a nuclear localization signal (underlined) and four mbt repeats (boldface and boxed). Alignment of the four mbt repeats of mouse Hemp to the consensus sequence is shown in Fig. 1*B* and the comparative structural characteristics of known mbt-containing proteins are shown in Fig. 1*C*. The mbt proteins are divided into two groups, depending on whether or not they possess an SPM (Scm, Ph, and MBT) domain, which mediates protein–protein interactions (12, 13). SPM-containing mbt proteins include D-L(3)mbt (7), H-L(3)mbt (8), SCMH1 (10), SCML2 (11), Sfmbt (Scm-related gene containing four mbt domains) (14), and MBT-1 (15) [shown as SPM(+) in Fig. 1*C*]; SPM-lacking mbt proteins include Hemp, h-L(3)mbt-like a (9), h-L(3)mbt-like b (9), and M4mbt (16) [shown as SPM(−) in Fig. 1*C*]. It is noteworthy that Hemp and other mbt-containing, SPM-lacking proteins share a structural similarity in that they contain four tandem mbt repeats preceded by a C2C2 zinc-finger domain [SPM(−) in Fig. 1*C*]. Therefore, these proteins may constitute a previously unexplored subfamily of mbt-containing proteins.

Because the expression of *hemp* mRNA in distinct hematopoietic lineages has been reported previously (6), in this study the expression patterns of *hemp* were examined in mouse tissues and in human hematopoietic and nonhematopoietic cell lines. The results are shown in Fig. 1*D*. In adult mouse tissues, *hemp* showed restricted expression, with high expression in the testis (*Top*). In human cell lines, *hemp* was expressed abundantly in most of the hematopoietic cell lines (*Middle*), and it exhibited weak expression in all of the nonhematopoietic cell lines, except

Author contributions: H.H., K.A.M., Z.-i.H., T.S., and I.R.L. designed research; H.H., K.T., H.O., K.K., T.T., N.Y., and K.M. performed research; H.H., K.T., H.O., K.K., T.T., N.Y., K.M., K.A.M., Z.-i.H., T.S., and I.R.L. analyzed data; and H.H., K.T., H.O., K.K., and K.M. wrote the paper.

The authors declare no conflict of interest.

This article is a PNAS Direct Submission.

[1]H.H. and K.T. contributed equally to this work.

[2]To whom correspondence should be addressed. E-mail: hhonda@hiroshima-u.ac.jp.

This article contains supporting information online at www.pnas.org/lookup/suppl/doi:10.1073/pnas.1003403108/-/DCSupplemental.

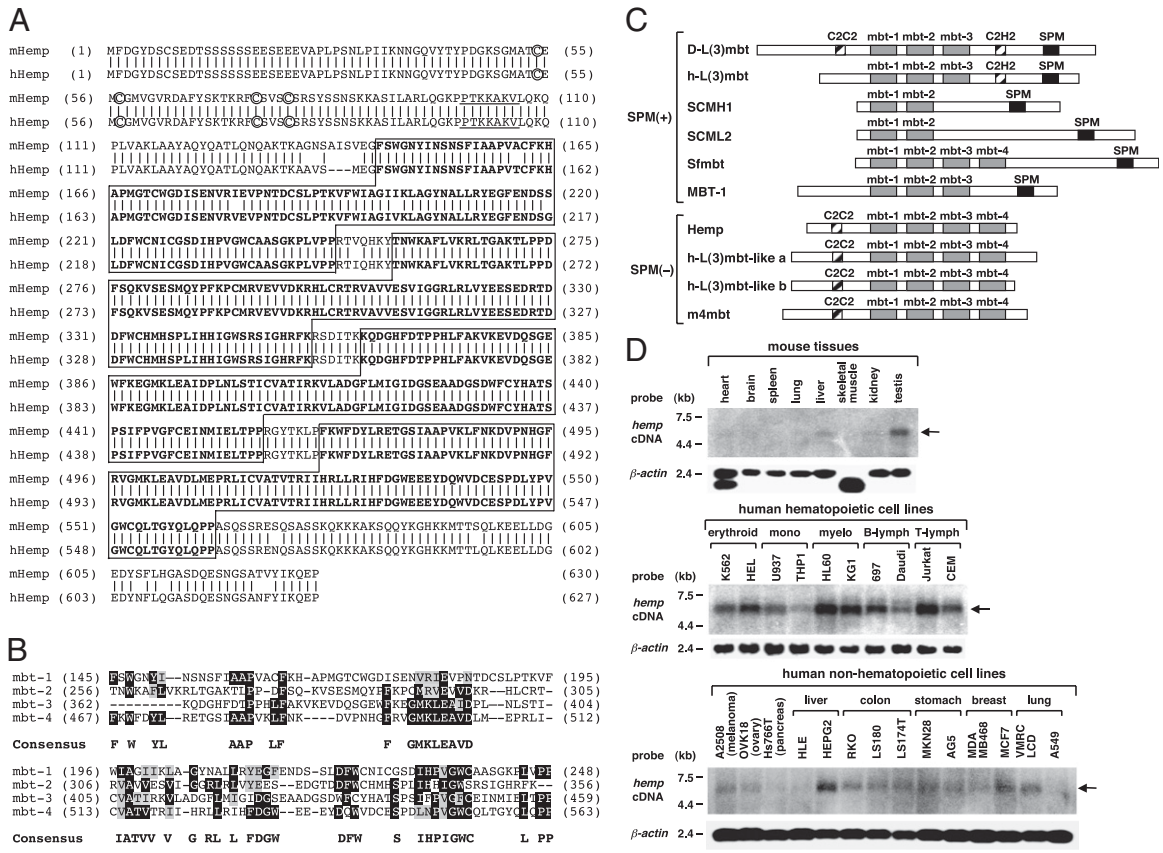

Fig. 1. Structure and expression of Hemp. (*A*) Comparison of amino acid sequences of mouse Hemp (*Upper*) and human Hemp (*Lower*) proteins. Vertical lines indicate identical amino acids. Zinc-finger domain cysteine residues are circled, a nuclear localization signal is underlined, and each of the four mbt repeats is shown in boldface surrounded by a box. (*B*) Alignment of the four mbt repeats of mouse Hemp with the mbt consensus sequences. Identical and similar amino acids to the consensus sequences are indicated by black and gray backgrounds, respectively. Amino acid numbers are shown in parentheses. (*C*) Comparison of the primary structures of previously reported mbt-containing proteins. The proteins are divided into two groups, SPM(+) and SPM(–), depending on whether or not they possess the SPM domain (shown as a black box). The mbt domain and the C2C2/C2HC Zinc-finger domain are indicated by gray and shaded boxes, respectively. (*D*) Expression of *hemp* RNA in mouse tissues and in human hematopoietic and nonhematopoietic cell lines. The position of *hemp* is indicated by an arrow. Hybridization with *β-actin* cDNA is shown as an internal control.

HEPG2 (*Bottom*). These results indicated that *hemp* is preferentially expressed in hematopoietic cell lines and suggested that Hemp functions largely in hematopoietic cells.

Neonatal Lethality and Skeletal Abnormalities in *hemp*$^{-/-}$ Mice. The *hemp*-deficient mice were generated by replacing the mbt-coding exons with *IRES-GFP-pA* and the *floxed Neo* resistance gene (Fig. S1*A*). As shown in Fig. S1 *B* and *C*, the *hemp* gene was correctly targeted and *hemp*-null mutant (*hemp*$^{-/-}$) mice were obtained.

No live homozygotes were found at 3-wk postnatal littermates [postnatal day (P) 21.5] (Table S1), indicating that *hemp*$^{-/-}$ mice die perinatally. To determine the time of lethality, embryos and neonates, obtained from timed *hemp*$^{+/-}$ intercrosses, were genotyped. At embryonic day (E) 12.5 and E17.5, *hemp*$^{+/+}$, *hemp*$^{+/-}$, and *hemp*$^{-/-}$ embryos were present almost at Mendelian ratios. However, at P0.5, numbers of *hemp*$^{-/-}$ pups decreased and most of them were found dead (Table S1). In addition, 1 d later, no live *hemp*$^{-/-}$ pups were obtained (Table S1), indicating that all *hemp*$^{-/-}$ neonates die by P1.5.

To investigate the cause of *hemp*$^{-/-}$ postnatal lethality, prenatal and neonatal mice were subjected to pathological analysis. However, despite intensive analysis, no obvious changes were detected in the internal organs of *hemp*$^{-/-}$ mice. The next step was to examine skeletal formation in *hemp*$^{-/-}$ mice, because previous studies showed that mice with deficiencies in several of the PcG proteins exhibited abnormal skeletal development (17). Representative whole-mount pictures of *hemp*$^{+/+}$, *hemp*$^{+/-}$, and *hemp*$^{-/-}$ embryos at E14.5 and E17.5 are shown in Fig. 2. At E14.5 (Fig. 2, *Upper Right*), *hemp*$^{-/-}$ embryos generally exhibited poor skeletal development, most noticeably, the cartilage primordium of the occipital bone at the base of the cranium (No. 1 and an arrow). In addition, insufficient formation of the atlas (C1) and the axis (C2) vertebrae (No. 2), a curvature of the spine (Nos. 3 and 5 in the right lower section), a misalignment of the spine (No. 4), and fusions of the cervical vertebrae [an arrowhead (C2 and C3 fusion), also shown by arrowheads in the right, upper, and center sections (C1 and C2 fusion and C1 to C3 fusion, respectively)] were found in *hemp*$^{-/-}$ embryos. At E17.5 (Fig. 2, *Lower Right*), the defects were more pronounced and various abnormalities were observed in *hemp*$^{-/-}$ embryos, especially in the cranium, vertebrae, and ribs. The most common and prominent feature in *hemp*$^{-/-}$ embryos was the short lambdoidal suture and flattened interparietal and occipital bones (Nos. 1 and 2). In addition, in the *hemp*$^{-/-}$ embryo presented in Fig. 2, the atlas (C1) vertebra is adjacent to the occipital bone, there is a prominent curvature of the spine at the seventh and eighth vertebrae (T7 and T8), and three ribs are attached to thoracic vertebra T7 and eight ribs to T8 (Nos. 3–6). Other skeletal malformations in *hemp*$^{-/-}$ embryos included fusions of cervical vertebrae [arrowheads in the right upper section (C3 and C4, and C5 and C6 fusions)], a fusion and a split at the first ribs (Fig. 2, *Right Center*, arrow), and the attachment of four ribs to the same vertebra and a deformity of the 12th rib (Fig. 2, *Right Lower*, arrow and arrowhead). No ob-

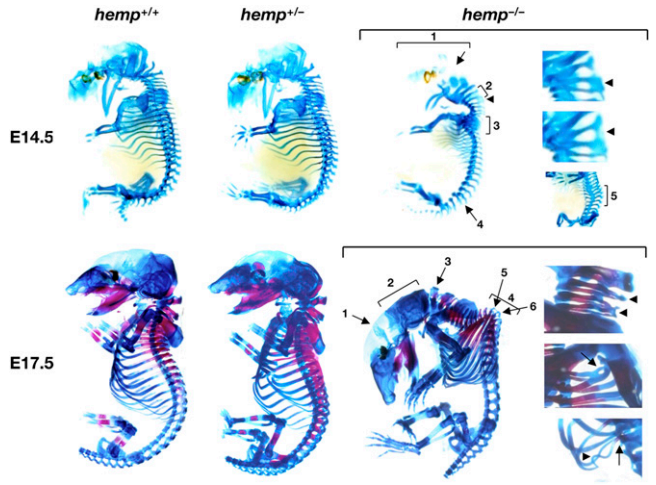

Fig. 2. Representative skeletal photographs of *hemp*$^{+/+}$ (*Left*), *hemp*$^{+/-}$ (*Center*), and *hemp*$^{-/-}$ (*Right*) embryos at E14.5 (*Upper*) and E17.5 (*Lower*). Abnormal skeletal features in *hemp*$^{-/-}$ embryos are indicated by arrows, arrowheads, and numbers.

vious alterations were found in other parts of the skeleton, such as the limbs. In addition, no abnormalities were found in *hemp*$^{+/-}$ embryos (Fig. 2, *Center*), indicating that a haplo-insufficiency of *hemp* does not cause skeletal abnormalities and there is no dosage effect of Hemp in skeletal development.

Reduction of Mononuclear Cells and HSCs in *hemp*$^{-/-}$ FL During Early Development. Because *hemp* was originally isolated from a highly enriched mouse FL HSC cDNA library, we investigated whether a Hemp deficiency affected embryonic hematopoiesis. *Hemp* expression levels were initially examined in the FL at E11.5, E14.5, and E18.5. As shown in Fig. S2*A*, *hemp* expression was highest at E11.5 and decreased thereafter. Next, the expression levels of *hemp* were examined at different stages of hematopoietic differentiation using the FL HSC marker, CD150 (18). Cells from E11.5, E14.5 and E18.5 FLs were separated into CD150^{+}, lineage marker (Lin)-negative, Sca-1^{+}, and c-Kit^{+} (LSK); CD150^{-} LSK (putative HSCs); progenitor, Lin^{-} and Lin^{+} cell fractions, and RNA, extracted from each fraction, was subjected to quantitative real-time PCR. As shown in Fig. S2*B*, at E11.5, *hemp* was expressed at roughly the same level in all four fractions, whereas at E14.5 and E18.5 it was predominantly expressed in the CD150^{+} and CD150^{-} LSK fractions. These results indicated that *hemp* is preferentially expressed in primitive hematopoietic cells, including HSCs, and may play a major role in these types of cells.

Next, cell numbers were examined in the FL of *hemp*$^{+/+}$ and *hemp*$^{-/-}$ embryos at E14.5 and E18.5. At E14.5, the FL sizes of *hemp*$^{-/-}$ embryos were significantly smaller than those in *hemp*$^{+/+}$ embryos. Thus, to ensure the recovery of HSCs at this time point, we collected FL cells without using lymphoprep gradients (Lymphoprep). On the other hand, at E18.5, because the FL sizes of *hemp*$^{-/-}$ and *hemp*$^{+/+}$ embryos were almost comparable, we separated FL mononuclear cells by using Lymphoprep. Our previous study demonstrated that the use of these two different methods (preparation with or without Lymphoprep) does not affect the characteristics of the isolated cells, in terms of surface markers, functional abilities, or number of HSCs (19). As shown in the left panels of E14.5 and E18.5 in Fig. 3*A*, at E14.5, *hemp*$^{-/-}$ FL cell numbers were reduced approximately twofold relative to controls (E14.5 of Fig. 3*A*, *Left*), whereas at E18.5, both *hemp*$^{+/+}$ and *hemp*$^{-/-}$ FLs contained comparable numbers of mononuclear cells (E18.5 of Fig. 3*A*, *Left*).

To investigate whether the reduction in cell numbers in the *hemp*$^{-/-}$ FL was caused by a differentiation block at a specific developmental stage, or by a proliferative defect of HSCs, flow cytometric analysis was performed using the lineage markers, Sca-1, c-Kit, CD150, and endothelial protein C receptor (EPCR), another marker for FL-HSCs (19). The absolute cell numbers per FL in each fraction are shown in E14.5 and E18.5 in Fig. 3*A Right*. The absolute LSK number in the *hemp*$^{-/-}$ FL was significantly reduced compared with that in the *hemp*$^{+/+}$ FL at both E14.5 and E18.5 (Fig. 3*A*, *Top Right*: E14.5 and E18.5). Regarding the HSC frequencies in the LSK fractions, *hemp*$^{-/-}$ FL showed a significant decrease in absolute cell numbers of CD150^{+} LSK and EPCR^{+} LSK fractions at E14.5 (Fig. 3*A*, *Right Middle*, and *Bottom*: E14.5). At E18.5, although the cell number of CD150^{+} LSK were still low in *hemp*$^{-/-}$ FL (Fig. 3*A*, *Right Middle*: E18.5), those of EPCR^{+} LSK were comparable between the two types of embryos (Fig. 3*A*, *Right Bottom*: E18.5). These results indicated that a deficiency in Hemp impairs HSC development, especially at an early developmental stage.

Impaired Proliferative and Repopulating Ability of *hemp*$^{-/-}$ HSCs. To test the functional properties of primitive *hemp*$^{-/-}$ hematopoietic cells, we first investigated the colony-forming units in culture (CFU-C) and then performed high proliferative potential colony-forming cell (HPP-CFC) assays, which reflect progenitor cell capacity, using E14.5 and E18.5 CD150^{+} LSK cells (Fig. 3 *B* and 3*C*). At E14.5, *hemp*$^{-/-}$ CD150^{+} LSK cells generated a significantly reduced number of colonies in both CFU-C and HPP-CFC assays compared with *hemp*$^{+/+}$ CD150^{+} LSK cells, indicating a marked decrease in the proliferative ability of *hemp*$^{-/-}$ HSCs (Fig. 3 *B* and 3*C*, *Left*). In contrast, at E18.5 no apparent differences were observed between the two assays (Fig. 3 *B* and 3*C*, *Right*). These results indicated that a Hemp deficiency impaired the proliferative potentials of hematopoietic stem/early progenitor cells at an early developmental stage.

Next, a competitive repopulation assay was performed to investigate the stem cell capacity of *hemp*$^{-/-}$ CD150^{+} LSK cells at E14.5. As shown in Fig. 4*C*, the repopulation capacity of *hemp*$^{-/-}$ CD150^{+} LSK cells was significantly reduced compared with *hemp*$^{+/+}$ CD150^{+} LSK cells, as indicated by a marked decrease in the percentages of donor-derived cells in peripheral blood (Fig. 3*D*, *Left*) and bone marrow (Fig. 3*D*, *Right*) in the recipient mice. These results demonstrated that a Hemp deficiency resulted in a severe functional defect of FL HSCs.

To gain mechanistic insights into HSC defects, the cell-cycle status and apoptotic ratios for CD150^{+} and CD150^{-} LSK cells from E14.5 and E18.5 FLs were examined. A significant reduction in short-term (90 min) BrdU incorporation was observed in CD150^{+} LSK cells from *hemp*$^{-/-}$ FL at E14.5 (Fig. S3*A*, *Left*), indicating increased cell-cycle arrest in this population. In addition, a marked increase in cleaved caspase-3–positive cells was detected in CD150^{+} and CD150^{-} LSK cells from *hemp*$^{-/-}$ FL at E14.5 (Fig. S3*B*, *Left*), indicating enhanced apoptosis in these cell populations. In contrast, At E18.5 these changes were attenuated and no significant differences were found (Fig. 3 *A* and *B*, *Right*). These results demonstrated that Hemp contributed significantly to the reconstitution ability of FL HSCs, potentially through the fine-tuning of the cell-cycle and cell-survival pathways.

Altered Gene-Expression Profiles in *hemp*$^{-/-}$ FL HSCs. To elucidate the detailed molecular mechanism underlying the impaired reconstitution ability of *hemp*$^{-/-}$ FL HSCs, we searched for genes whose expression levels were altered in FL HSCs by the Hemp deficiency. Total RNAs extracted from the lin^{-}/c-kit^{high} HSC-enriched fraction of E12.5 *hemp*$^{+/+}$ and *hemp*$^{-/-}$ FLs were subjected to microarray analysis. Among 23,522 genes examined, 308 genes were identified that exhibited absolute expression levels of more than 50 (*SI Materials and Methods*) in either *hemp*$^{+/+}$ or *hemp*$^{-/-}$ arrays, and showed alterations in expression of more than 1.5-fold between the two genotypes. Gene names are listed in Table S2 (>1.5-fold up-regulated in *hemp*$^{-/-}$ compared with *hemp*$^{+/+}$) and Table S3 (>1.5-fold down-regulated in *hemp*$^{-/-}$ compared with *hemp*$^{+/+}$), along with additional information concerning each gene. The marked reduction of *mbtd1* (=*hemp*) in the *hemp*$^{-/-}$ arrays verified the quantitative accuracy of the analysis (top row of Table S3). Of the 308 genes, 210 and 229

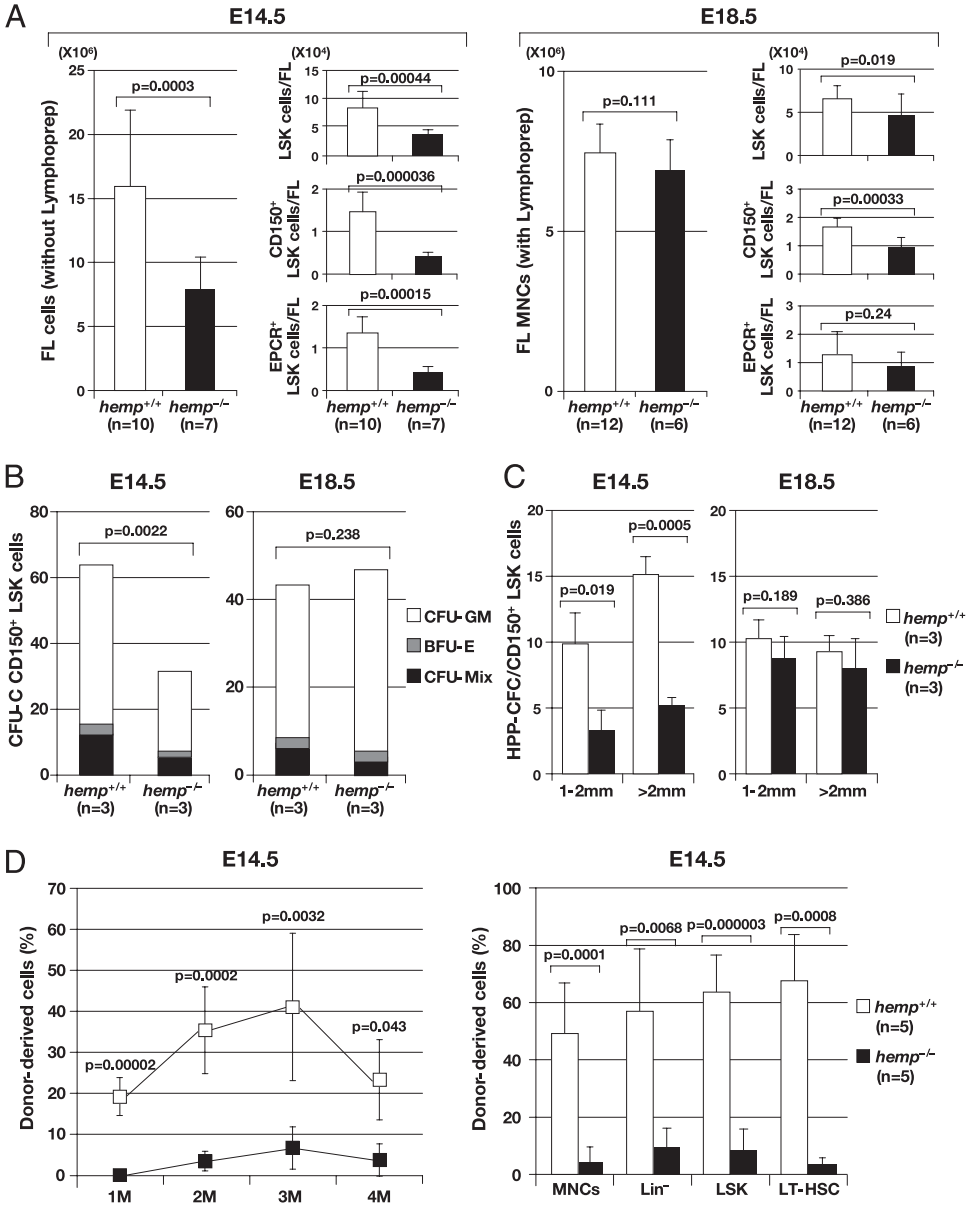

Fig. 3. Phenotypic characterization and functional assays of *hemp*$^{+/+}$ and *hemp*$^{-/-}$ FL cells. (*A*) Comparison of total cell numbers (*Left*) and absolute cell numbers for LSK (*Right Top*) CD150^{+} LSK (*Right, Middle*) and EPCR^{+} LSK (*Right, Bottom*) fractions between *hemp*$^{+/+}$ and *hemp*$^{-/-}$ FLs at E14.5 and E18.5 (data ± SD). At E14.5, FL cells were collected without using lymphoprep gradients (Lymphoprep), whereas at E18.5, FL mononuclear cells (MNCs) were separated with the use of Lymphoprep. (*B*) Average numbers of colony forming units in culture (CFU-C) generated from *hemp*$^{+/+}$ and *hemp*$^{-/-}$ CD150^{+} LSK cells at E14.5 and E18.5. One hundred and fifty cells were cultured for 8 d in a semi-solid culture with cytokines, and the colony types formed were classified into colony-forming unit-granulocyte, macrophage [(CFU-GM) open bar], burst-forming unit-erythroid [(BFU-E) gray bar], CFU-Mix (closed bar) and counted (data ± SD). (*C*) Average numbers of high proliferative potential-colony forming cells (HPP-CFCs) generated from *hemp*$^{+/+}$ (open bar) and *hemp*$^{-/-}$ (closed bar) CD150^{+} LSK cells at E14.5 and E18.5. One hundred and fifty cells were cultured for 16 d in a semi-solid culture with cytokines, and colonies from 1–2 mm and >2 mm were classified and counted independently (data ± SD). (*D*) Competitive repopulation assay of *hemp*$^{+/+}$ (open box) and *hemp*$^{-/-}$ (closed box) CD150^{+} LSK cells at E14.5. One hundred and fifty cells (Ly5.2) were transplanted into recipient mice (Ly5.1) together with 4×10^{5} competitors (Ly5.1). Donor-derived chimerism in the peripheral blood (PB) at 1, 2, 3 and 4 months after transplantation and chimerism in the MNC, Lin^{-}, LSK and LT-HSC fractions in the bone marrow (BM) at 4 mo after transplantation are shown in the left and right panels, respectively (data ± SD).

genes were classified according to "Biological process" and "Molecular function" Gene Ontology (GO) annotation, respectively (Fig. S4*A*).

Among the 308 genes, 39 genes were further selected based on their greater than twofold expression differences between the *hemp*$^{+/+}$ and *hemp*$^{-/-}$ arrays. The gene names, classified according to the GO category and expression-difference ratios are listed in Table 1 and the actual gene-expression levels in *hemp*$^{+/+}$ and *hemp*$^{-/-}$ arrays are shown in Fig. S4*B*. Interestingly, these genes included those reported to play important roles in hematopoietic development and HSC reconstitution ability, as discussed below.

Discussion

In this study, we generated mice deficient in Hemp, an mbt-encoding protein, and found that a loss of Hemp induced severe abnormalities in HSC function and skeletal formation.

To investigate whether these abnormalities were caused directly by the Hemp deficiency, Hemp expression patterns during embryogenesis were examined using an anti-Hemp antibody. As shown in Fig. S5, various tissues were stained positively at E11.5 and E14.5 (Fig. S5, *Left*). The liver and cartilage, where phenotypical and functional abnormalities were found in *hemp*$^{-/-}$ embryos, were examined in detail. In the liver, interstitial cells, including hematopoietic cells, showed positive staining; and in the cartilage, most of the chondrocytes and some undifferentiated mesenchymal cells exhibited positive signals (Fig. S5, *Right*: E11.5 and E14.5). These results strongly suggested that the defects in *hemp*$^{-/-}$ embryos were primarily attributed to the Hemp deficiency. The reason for the lack of obvious defects in other tissues expressing Hemp, such as the heart (Fig. S5), is not yet clear. One possibility is that Hemp-related proteins (Fig. 1*C*) might compensate for Hemp function in these tissues.

The skeletal abnormalities were considered to be responsible for the postnatal lethality of the *hemp*$^{-/-}$ mice. The impaired thoracic formation would cause respiratory failure, lead to hypoxia, and eventually result in neonatal death. Skeletal malformations are one of the characteristic abnormalities in mice lacking several of the *PcG* genes, such as *bmi-1* (20), *mel-18* (21), and *M33* (22). However, these mice exclusively displayed anterior/posterior homeotic transformations of vertebrae because of the ectopic or deregulated expression of *Hox* gene families (17), in contrast to *hemp*$^{-/-}$ mice, which exhibited very complex patterns that did not correspond to the homeotic transformations

Table 1. Genes with expression levels showing greater than a twofold difference between *hemp*$^{+/+}$ and *hemp*$^{-/-}$ arrays

Category	Gene symbol	Global normalization ratio
Transcription	***Prdm16***	**2.3↑**
	Sox4	0.5↓
	Zmynd11	0.5↓
	Stat4	0.5↓
	Hnrnpul1	0.4↓
Signal transduction	***Arhgap21***	**4.1↑**
	Eltd1	0.4↓
	Arhgef18	0.4↓
	Olfr1461	0.4↓
Metabolic process	*Acot2*	0.5↓
	Sepp1	0.5↓
	Aqp9	0.4↓
	Pitpnc1	0.3↓
Translation	***Eif2s3y***	**2.3↑**
	Aars2	0.4↓
Oxygen transport	*Hbb-b1*	0.5↓
	Hba-a1	0.4↓
Immune response	*Ccl4*	0.4↓
	Cxcl2	0.4↓
Chemotaxis	***Ear2***	**2.2↑**
Protein folding	***Fkbp11***	**2.1↑**
Apoptosis	*Nfkbia*	0.5↓
Others	***Dcdc5***	**4.4↑**
	Evc2	**3.9↑**
	Acbd7	**3.3↑**
	Adamtsl1	**2.9↑**
	Ear1	**2.2↑**
	Ear10	**2.1↑**
	Tlcd2	**2.0↑**
	Ear6	**2.0↑**
	Dolpp1	0.5↓
	EG625796	0.5↓
	Slc6a20a	0.4↓
	Gal3st2	0.4↓
	Erdr1	0.4↓
	Dusp2	0.4↓
	Xist	0.3↓
	Lelp1	0.3↓
	Mboat2	0.3↓

Genes with a greater than twofold increase in expression in *hemp*$^{-/-}$ arrays are shown in boldface.

(Fig. 2). Therefore, Hemp appears to regulate skeletal development in a manner distinct from that of the PcG proteins.

Interestingly, the cervical vertebral fusion and an atlas (C1) vertebra located adjacent to the occipital bone (common skeletal abnormalities in *hemp*$^{-/-}$ mice) closely resembled the features of the Klippel-Feil anomaly in humans (23, 24). In addition, rib anomalies are frequently associated with this disease (25). The Klippel-Feil anomaly is etiologically heterogeneous, but several cases bear chromosomal aberrations and thus are considered to have a genetic component (26, 27). Of note, one case with Klippel-Feil anomaly had a translocation involving chromosome band 17q23 (26), which is close to the human *hemp* orthologous locus at 17q21.3. In addition, several patients with unrelated skeletal abnormalities were shown to bear chromosomal aberrations involving 17q21.3 (28–30). Therefore, it would be intriguing to investigate whether human *hemp* expression is affected in patients with Klippel-Feil anomaly and patients with skeletal abnormalities carrying chromosomal aberrations involving 17q21.3.

In the hematopoietic analyses, we observed a significant reduction in FL cell numbers in *hemp*$^{-/-}$ embryos at E14.5 (Fig. 3*A*). Flow cytometric analysis revealed that the reduction occurred at the HSC level (Fig. 3*A*), demonstrating a critical role for Hemp in HSC development at an early developmental phase and leading to further investigations into the proliferative and repopulating abilities of HSCs. CFU-C and HPP-CFC assays of CD150^{+} LSK cells revealed that *hemp*$^{-/-}$ HSCs exhibited a significantly reduced proliferative ability at E14.5 (Fig. 3 *B* and *C*). In addition, transplantation of CD150^{+} LSK cells at E14.5 revealed a marked impairment in the repopulating activity of *hemp*$^{-/-}$ HSCs (Fig. 3*D*). These results indicated that Hemp plays a pivotal role, not only in hematopoietic development, but also in HSC proliferative and repopulating abilities. The BrdU and cleaved caspase-3 assays revealed significantly decreased proliferation and significantly enhanced apoptosis of *hemp*$^{-/-}$ CD150^{+} LSK cells at E14.5 (Fig. S3 *A* and *B*), which would explain, at least partly, the defects in *hemp*$^{-/-}$ HSCs. The reason why the defects in *hemp*$^{-/-}$ HSCs were most prominent at E14.5 but were less remarkable at E18.5 is not clear. One possibility is that *hemp* expression in the FL is highest at E11.5 and is down-regulated thereafter (Fig. S2*A*). However, at E18.5, *hemp* expression in the CD150^{+} and CD150^{-} LSK fractions remained dominant (Fig. S2*B*). Thus, the decline of the overall *hemp* expression in the FL at a later stage of development could be attributed to decreased *hemp* expression in Lin^{-} and Lin^{+} fractions at E18.5, because these cell types expand massively and occupy the majority of FL cells. Another, more likely, possibility is that Hemp-related molecules (Fig. 1*C*) may compensate for the defects of Hemp deficiency during late gestation.

To gain insights into the molecular mechanisms underlying the impaired hematopoietic activities of *hemp*$^{-/-}$ HSCs, a microarray analysis was performed. Among 23,522 genes examined, 39 genes were identified whose expression levels differed by more than twofold in enriched *hemp*$^{+/+}$ or *hemp*$^{-/-}$ stem and progenitor cell arrays (Table 1 and Fig. S4*B*), which included genes that have been shown to play pivotal roles in HSC self-renewal capacity and differentiation ability.

Among genes down-regulated in *hemp*$^{-/-}$ FL HSCs, *Sox4* (0.5) is necessary for lymphocyte development (31, 32) (the figure in parenthesis refers to the ratio of *hemp*$^{-/-}$/*hemp*$^{+/+}$, in this case, a value of 0.5). Of the two *Stat* genes identified, *Stat4* (0.5) is required for T-cell differentiation (33), and *Stat3* (0.6) plays important functions in HSC self-renewal (34). *KLF6* (0.6) is required for proper hematopoietic development (35), two of the chemokine family members, *Ccl4* (0.4) and *Cxcl2* (0.4), contribute to proliferation, survival and homing of hematopoietic cells (36), and *Erdr1* (0.4) is capable of inducing hemoglobin synthesis (37). Among the genes up-regulated in *hemp*$^{-/-}$ FL HSC and progenitor cells, *SOCS2* (1.7) negatively regulates cytokine-mediated pathways (38) and *MAP4K1* (1.8) induces apoptosis by activating MAP3 proteins and suppressing Bcl2 family members (39, 40). Taken together, the altered expression patterns of various genes in mutant FL HSCs appear to coordinately and cooperatively impair the expansion and reconstitution ability of FL HSCs.

Recently, a functional screen for gene products supporting HSC activity identified 18 molecules, and the overexpression of 10 of these was shown to increase HSC repopulating activity (41). Interestingly, 3 of the 10 genes overlapped with the 39 genes identified in this study (Table 1 and Fig. S4*B*). Two of these were *Sox4* and *Erdr1*, which were down-regulated in *hemp*$^{-/-}$ FL HSCs (0.5 and 0.4, respectively) (Table 1 and Fig. S4*B*). Therefore, it is strongly postulated that the suppressed expression of these two gene products is responsible for the impaired reconstitution ability of *hemp*$^{-/-}$ FL HSCs. The third gene, *Prdm16* (also known as *Mel1*), was up-regulated in *hemp*$^{-/-}$ FL HSCs (2.3) (Table 1 and Fig. S4*B*). This finding is intriguing, because *Prdm16* was originally isolated as a leukemia-associated gene (42) and is known to enhance HSC activity (41). The mechanism underlying the enhanced expression of *Prdm16* remains unclear, but one possibility is that *Prdm16* is up-regulated to compensate for the impaired proliferative ability of FL HSCs induced by Hemp deficiency.

In summary, we have demonstrated that Hemp, an mbt-containing protein, plays essential roles in HSC function and skeletal formation. Recent studies have shown that the mbt domain binds to methylated histone residues, for example, the mbt domain of H-L(3)MBT/L3MBTL1 binds to methylated H3K4

and H4K20 (43, 44) and also compacts nucleosomal arrays by simultaneously binding to two methylated residues, H4K20 and H1bK26 (45). In addition, Sfmbt binds to mono- and dimethylated H3K9 and H4K20 (46, 47), and its gene-silencing activity is enhanced by interacting with another mbt-containing protein, Scm (48). Therefore, it is likely that Hemp exerts its biological activity by binding to methylated histone lysine residues through the mbt repeats. Further studies will be required to clarify the lysine residues to which Hemp binds and the proteins with which Hemp interacts. In addition, an association between skeletal anomalies and impaired hematopoiesis has been reported in human diseases (49), and in particular, the Klippel-Feil anomaly can be associated with Fanconi anemia (50) and Diamond-Blackfan syndrome (51, 52). Therefore, it will be interesting to determine whether human Hemp dysfunctions are involved in the pathogenesis of these diseases.

Materials and Methods

Detailed descriptions for experimental procedures for Northern blot analysis, construction of a targeting vector and generation of *hemp* knockout mice, generation of an anti-Hemp antibody, immunoprecipitation and Western blot analysis, skeletal analysis, quantitative real-time PCR, immunohistochemical analysis, flow cytometric analysis, CFU-C, HPP-CFC and competitive repopulation assays, cell cycle and apoptosis assays, and DNA microarray analysis, microarray scanning and data processing are provided in *SI Materials and Methods*.

ACKNOWLEDGMENTS. We thank Yuki Sakai, Kayoko Hashimoto, Yuko Tsukawaki, Tai Rika, and Tomoko Muraki for the mouse care and technical assistance, and Masaaki Miyazaki for help in preparing specimens and hematopoietic analysis, Toshikazu Ushijima for providing us with non-hematopoietic cell lines, and Tetsuo Sudo and Hideo Akiyama from Toray Co., Ltd. for microarray analysis. This work was supported by a Grant-in-Aid from the Ministry of Education, Science and Culture of Japan, a Grant-in-Aid for Cancer Research from the Ministry of Health, Labour and Welfare of Japan (13-2), and a Human Frontier Science Program Organization Long-Term Fellowship.

1. Lemischka IR, Raulet DH, Mulligan RC (1986) Developmental potential and dynamic behavior of hematopoietic stem cells. *Cell* 45:917–927.
2. Osawa M, Hanada K, Hamada H, Nakauchi H (1996) Long-term lymphohematopoietic reconstitution by a single CD34-low/negative hematopoietic stem cell. *Science* 273: 242–245.
3. Akala OO, Clarke MF (2006) Hematopoietic stem cell self-renewal. *Curr Opin Genet Dev* 16:496–501.
4. Zon LI (2008) Intrinsic and extrinsic control of haematopoietic stem-cell self-renewal. *Nature* 453:306–313.
5. Dzierzak E, Speck NA (2008) Of lineage and legacy: The development of mammalian hematopoietic stem cells. *Nat Immunol* 9:129–136.
6. Phillips RL, et al. (2000) The genetic program of hematopoietic stem cells. *Science* 288: 1635–1640.
7. Wismar J, et al. (1995) The *Drosophila melanogaster* tumor suppressor gene lethal(3) malignant brain tumor encodes a proline-rich protein with a novel zinc finger. *Mech Dev* 53:141–154.
8. Koga H, et al. (1999) A human homolog of *Drosophila* lethal(3)malignant brain tumor (l(3) mbt) protein associates with condensed mitotic chromosomes. *Oncogene* 18:3799–3809.
9. Wismar J (2001) Molecular characterization of h-l(3)mbt-like: A new member of the human mbt family. *FEBS Lett* 507:119–121.
10. Berger J, et al. (1999) The human homolog of Sex comb on midleg (SCMH1) maps to chromosome 1p34. *Gene* 237(1):185–191.
11. Montini E, et al. (1999) Identification of SCML2, a second human gene homologous to the *Drosophila* sex comb on midleg (Scm): A new gene cluster on Xp22. *Genomics* 58:65–72.
12. Bornemann D, Miller E, Simon J (1996) The *Drosophila* Polycomb group gene Sex comb on midleg (Scm) encodes a zinc finger protein with similarity to polyhomeotic protein. *Development* 122:1621–1630.
13. Peterson AJ, et al. (1997) A domain shared by the Polycomb group proteins Scm and ph mediates heterotypic and homotypic interactions. *Mol Cell Biol* 17:6683–6692.
14. Usui H, Ichikawa T, Kobayashi K, Kumanishi T (2000) Cloning of a novel murine gene *Sfmbt*, Scm-related gene containing four mbt domains, structurally belonging to the Polycomb group of genes. *Gene* 248(1-2):127–135.
15. Arai S, Miyazaki T (2005) Impaired maturation of myeloid progenitors in mice lacking novel Polycomb group protein MBT-1. *EMBO J* 24:1863–1873.
16. Markus J, Feiková S, Sramko M, Wolff L, Bies J (2003) Proliferation-linked expression of the novel murine gene m4mbt encoding a nuclear zinc finger protein with four mbt domains. *Gene* 319:117–126.
17. van Lohuizen M (1998) Functional analysis of mouse Polycomb group genes. *Cell Mol Life Sci* 54:71–79.
18. Kim I, He S, Yilmaz OH, Kiel MJ, Morrison SJ (2006) Enhanced purification of fetal liver hematopoietic stem cells using SLAM family receptors. *Blood* 108:737–744.
19. Iwasaki H, Arai F, Kubota Y, Dahl M, Suda T (2010) Endothelial protein C receptor-expressing hematopoietic stem cells reside in the perisinusoidal niche in fetal liver. *Blood* 116:544–553.
20. van der Lugt NM, et al. (1994) Posterior transformation, neurological abnormalities, and severe hematopoietic defects in mice with a targeted deletion of the bmi-1 proto-oncogene. *Genes Dev* 8:757–769.
21. Akasaka T, et al. (1996) A role for mel-18, a Polycomb group-related vertebrate gene, during theanteroposterior specification of the axial skeleton. *Development* 122: 1513–1522.
22. Coré N, et al. (1997) Altered cellular proliferation and mesoderm patterning in Polycomb-M33-deficient mice. *Development* 124:721–729.
23. Klimo P, Jr., Rao G, Brockmeyer D (2007) Congenital anomalies of the cervical spine. *Neurosurg Clin N Am* 18:463–478.
24. Smoker WR, Khanna G (2008) Imaging the craniocervical junction. *Childs Nerv Syst* 24: 1123–1145.
25. Baga N, Chusid EL, Miller A (1969) Pulmonary disability in the Klippel-Feil syndrome. A study of two siblings. *Clin Orthop Relat Res* 67:105–110.
26. Fukushima Y, et al. (1995) De novo apparently balanced reciprocal translocation between 5q11.2 and 17q23 associated with Klippel-Feil anomaly and type A1 brachydactyly. *Am J Med Genet* 57:447–449.
27. Goto M, Nishimura G, Nagai T, Yamazawa K, Ogata T (2006) Familial Klippel-Feil anomaly and t(5;8)(q35.1;p21.1) translocation. *Am J Med Genet* 140:1013–1015.
28. Yue Y, et al. (2007) De novo t(12;17)(p13.3;q21.3) translocation with a breakpoint near the 5′ end of the HOXB gene cluster in a patient with developmental delay and skeletal malformations. *Eur J Hum Genet* 15:570–577.
29. Rooryck C, et al. (2008) A 580 kb microdeletion in 17q21.32 associated with mental retardation, microcephaly, cleft palate, and cardiac malformation. *Eur J Med Genet* 51:74–80.
30. Zahir FR, et al. (2009) A novel de novo 1.1 Mb duplication of 17q21.33 associated with cognitive impairment and other anomalies. *Am J Med Genet* 149A:1257–1262.
31. Schilham MW, et al. (1996) Defects in cardiac outflow tract formation and pro-B-lymphocyte expansion in mice lacking Sox-4. *Nature* 380:711–714.
32. Schilham MW, Moerer P, Cumano A, Clevers HC (1997) Sox-4 facilitates thymocyte differentiation. *Eur J Immunol* 27:1292–1295.
33. Kaplan MH, Sun YL, Hoey T, Grusby MJ (1996) Impaired IL-12 responses and enhanced development of Th2 cells in Stat4-deficient mice. *Nature* 382:174–177.
34. Hankeys PA (2009) Regulation of hematopoietic cell development and function by Stat3. *Front Biosci* 1:5273–5290.
35. Matsumoto N, et al. (2006) Developmental regulation of yolk sac hematopoiesis by Kruppel-like factor 6. *Blood* 107:1357–1365.
36. Broxmeyer HE (2001) Regulation of hematopoiesis by chemokine family members. *Int J Hematol* 74:9–17.
37. Dörmer P, Spitzer E, Frankenberger M, Kremmer E (2004) Erythroid differentiation regulator (EDR), a novel, highly conserved factor I. Induction of haemoglobin synthesis in erythroleukaemic cells. *Cytokine* 26:231–242.
38. Krebs DL, Hilton DJ (2001) SOCS proteins: Negative regulators of cytokine signaling. *Stem Cells* 19:378–387.
39. Brenner D, et al. (2007) Caspase-cleaved HPK1 induces CD95L-independent activation-induced cell death in T and B lymphocytes. *Blood* 110:3968–3977.
40. Shui JW, et al. (2007) Hematopoietic progenitor kinase 1 negatively regulates T cell receptor signaling and T cell-mediated immune responses. *Nat Immunol* 8:84–91.
41. Deneault E, et al. (2009) A functional screen to identify novel effectors of hematopoietic stem cell activity. *Cell* 137:369–379.
42. Mochizuki N, et al. (2000) A novel gene, *MEL1*, mapped to 1p36.3 is highly homologous to the *MDS1/EVI1* gene and is transcriptionally activated in t(1;3)(p36; q21)-positive leukemia cells. *Blood* 96:3209–3214.
43. Kim JY, et al. (2006) Tudor, MBT and chromo domains gauge the degree of lysine methylation. *EMBO Rep* 7:397–403.
44. Min J, et al. (2007) L3MBTL1 recognition of mono- and dimethylated histones. *Nat Struct Mol Biol* 14:1229–1230.
45. Trojer P, et al. (2007) L3MBTL1, a histone-methylation-dependent chromatin lock. *Cell* 129:915–928.
46. Klymenko T, et al. (2006) A Polycomb group protein complex with sequence-specific DNA-binding and selective methyl-lysine-binding activities. *Genes Dev* 20:1110–1122.
47. Guo Y, et al. (2009) Methylation-state-specific recognition of histones by the MBT repeat protein L3MBTL2. *Nucleic Acids Res* 37:2204–2210.
48. Grimm C, et al. (2009) Molecular recognition of histone lysine methylation by the Polycomb group repressor dSfmbt. *EMBO J* 28:1965–1977.
49. Charles JE, Robert PE, Anthony WB (2008) *Inborn Errors of Development* (Oxford University Press, Oxford, United Kingdom), 2nd Ed.
50. McGaughran J (2003) Klippel-Feil anomaly in Fanconi anemia. *Clin Dysmorphol* 12(3):197.
51. Greenspan A, Cohen J, Szabo RM (1991) Klippel-Feil syndrome. An unusual association with Sprengel deformity, omovertebral bone, and other skeletal, hematologic, and respiratory disorders. A case report. *Bull Hosp Jt Dis Orthop Inst* 51(1):54–62.
52. Lazarus KH, McCurdy FA (1984) Multiple congenital anomalies in a patient with Diamond-Blackfan syndrome. *Clin Pediatr (Phila)* 23:520–521.